Luminescence | *Very Important Paper*

VIP Nitridophosphate-Based Ultra-Narrow-Band Blue-Emitters: Luminescence Properties of $AEP_8N_{14}:Eu^{2+}$ (AE = Ca, Sr, Ba)

Sebastian Wendl,[a] Lucien Eisenburger,[a, b] Philipp Strobel,[c] Daniel Günther,[b] Jonathan P. Wright,[d] Peter J. Schmidt,[c] Oliver Oeckler,[b] and Wolfgang Schnick*[a]

Abstract: The nitridophosphates AEP_8N_{14} (AE = Ca, Sr, Ba) were synthesized at 4–5 GPa and 1050–1150 °C applying a 1000 t press with multianvil apparatus, following the azide route. The crystal structures of CaP_8N_{14} and SrP_8N_{14} are isotypic. The space group *Cmcm* was confirmed by powder X-ray diffraction. The structure of BaP_8N_{14} (space group *Amm*2) was elucidated by a combination of transmission electron microscopy and diffraction of microfocused synchrotron radiation. Phase purity was confirmed by Rietveld refinement. IR spectra are consistent with the structure models and the chemical compositions were confirmed by X-ray spectroscopy. Luminescence properties of Eu^{2+}-doped samples were investigated upon excitation with UV to blue light. CaP_8N_{14} (λ_{em} = 470 nm; fwhm = 1380 cm^{-1}) and SrP_8N_{14} (λ_{em} = 440 nm; fwhm = 1350 cm^{-1}) can be classified as the first ultra-narrow-band blue-emitting Eu^{2+}-doped nitridophosphates. BaP_8N_{14} shows a notably broader blue emission (λ_{em} = 417/457 nm; fwhm = 2075/3550 cm^{-1}).

Introduction

The importance of advanced, highly efficient phosphor materials is continuously growing, as phosphor-converted light-emitting diodes (pc-LEDs) have revolutionized the global lighting market with increased durability, colour rendering and enormous energy savings. This technique uses blue-emitting primary LEDs, mostly based on InGaN, which are coated with phosphors to achieve emission of white light by colour mixing. Demands on potential coatings are manifold and reach from chemical and thermal stability, efficient absorption of blue light (primary LED) over optical transparency and a small Stokes shift to high quantum efficiency and low thermal quenching.[1]

The most common coating for pc-LEDs is the oxide phosphor YAG:Ce ($Y_{3-x}Gd_xAl_{5-x}Ga_yO_{12}:Ce^{3+}$).[2,3] Eu^{2+}-doped nitrides, however, show intense broad-band emission upon excitation with UV to blue light due to the parity-allowed $4f^65d^1 \rightarrow 4f^7(^8S_{7/2})$ transition. (Oxo)nitridosilicates especially, have turned out to meet the above listed demands. $AESi_2O_2N_2:Eu^{2+}$, $AE_2Si_5N_8:Eu^{2+}$, and the so far narrowest nitride-based Eu^{2+} red emitter $Sr[Mg_3SiN_4]:Eu^{2+}$ have to be mentioned in this context.[4–8] Over the years, research on new phosphors expanded to a range of related compound classes, such as nitridoalumosilicates and nitridolithoaluminates, with $Ca[AlSiN_3]:Eu^{2+}$ and $Sr[LiAl_3N_4]:Eu^{2+}$ showing highly efficient red emission.[9,10] Recently, beryllium-containing nitrides have been shown to feature extremely narrow-band emissions in the blue to cyan spectral region.[11–13]

Nitridophosphates have repeatedly been discussed as phosphor materials as well, but only very few examples are known so far. The corresponding crystal structures are built up from anionic PN_4 tetrahedra networks that host the cations.[14] Among ternary all-nitride representatives, only $AEP_2N_4:Eu^{2+}$ (AE = Ca, Sr, Ba) and $Sr_3P_3N_7:Eu^{2+}$ are known.[15,16] However, these few members illustrate the versatility of nitridophosphates, as they cover a major part of the visible spectrum (λ_{emi} = 450–680 nm) and also feature high quantum efficiencies even for non-optimized powder samples.[15–18] The great potential of nitridophosphates is underlined by zeolite-like compounds $Ba_3P_5N_{10}X:Eu^{2+}$ (X = Cl, Br, I), of which $Ba_3P_5N_{10}Br:Eu^{2+}$ has to be highlighted, as it has been discussed as a natural-white-light single emitter.[17,18]

Fundamental research on nitridophosphates has established various synthetic approaches as recently reviewed in litera-

[a] S. Wendl, L. Eisenburger, Prof. Dr. W. Schnick
Department of Chemistry
University of Munich (LMU)
Butenandtstr. 5–13, 81377 München (Germany)
E-mail: wolfgang.schnick@uni-muenchen.de

[b] L. Eisenburger, D. Günther, Prof. Dr. O. Oeckler
Institute for Mineralogy, Crystallography and Material Science
Leipzig University
Scharnhorststr. 20, 04275 Leipzig (Germany)

[c] Dr. P. Strobel, Dr. P. J. Schmidt
Lumileds Phosphor Center Aachen (LPCA)
Lumileds (Germany) GmbH
Philipsstr. 8, 52068 Aachen (Germany)

[d] Dr. J. P. Wright
ESRF—The European Synchrotron
71 avenue des Martyrs, 38000 Grenoble (France)

Supporting information and the ORCID identification number(s) for the author(s) of this article can be found under:
https://doi.org/10.1002/chem.202001129.

© 2020 The Authors. Published by Wiley-VCH Verlag GmbH & Co. KGaA. This is an open access article under the terms of Creative Commons Attribution NonCommercial-NoDerivs License, which permits use and distribution in any medium, provided the original work is properly cited, the use is non-commercial and no modifications or adaptations are made.

ture.[14] Alkaline earth nitridophosphates are commonly prepared in high-pressure high-temperature reactions starting from P_3N_5 and the respective alkaline earth azide.[17–20] High-pressure conditions prevent the thermal decomposition of P_3N_5 that otherwise starts at 850 °C and high-temperature enables the reversible cleavage and formation of P–N bonds.[21]

In our previous work, we have reported on synthesis of highly condensed SrP_8N_{14} following the azide route.[20] Considering its crystal structure, which features octahedrally coordinated Sr atom sites, SrP_8N_{14} and structurally related compounds appear as candidates for promising luminescence properties. In this contribution, we expand the AEP_8N_{14} system by the new compounds CaP_8N_{14} and BaP_8N_{14}, and discuss structural relations within this series of nitridophosphates. Furthermore, we present intriguing luminescence properties of all three Eu^{2+}-doped compounds that classify AEP_8N_{14}:Eu^{2+} as the first P/N-based ultra-narrow-band blue-light emitters.

Results and Discussion

Synthesis

The nitridophosphates AEP_8N_{14} (AE = Ca, Sr, Ba) were synthesized by high-pressure high-temperature reactions at 4–5 GPa and 1050–1150 °C, using a modified Walker-type multianvil apparatus.[22–26] The syntheses follow the azide route, starting from P_3N_5 and the respective metal azide (Equation (1)). In order to investigate luminescence properties, Eu^{2+}-doped samples were obtained by addition of minor amounts of $EuCl_2$ (≈3 mole%) to the mixture of starting materials.

$$8\,P_3N_5 + 3\,AE(N_3)_2 \rightarrow 3\,AEP_8N_{14} + 8\,N_2 \quad (AE = \text{Ca, Sr, Ba}) \qquad (1)$$

White (AEP_8N_{14}) and yellowish (AEP_8N_{14}:Eu^{2+}) products have been formed as microcrystalline powders and appeared stable against treatment with air and water (Figure 1).

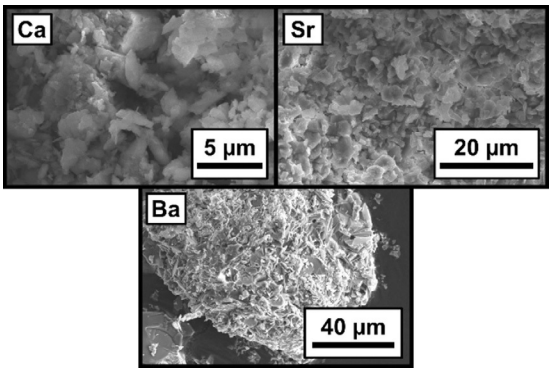

Figure 1. SEM images of AEP_8N_{14}:Eu^{2+} (AE = Ca, Sr, Ba), illustrating the microcrystalline character of the samples.

Structure elucidation

Owing to the lack of suitable single crystals, the structure of CaP_8N_{14} was refined from powder X-ray diffraction data employing the Rietveld method, where the published structure model of SrP_8N_{14} served as starting model (Figure 2).[20] The Rietveld method was further used to confirm phase purity of obtained SrP_8N_{14} (Figure 2). During refinement all atoms were refined with isotropic displacement parameters, using equal values for P and N atoms, respectively. Atomic coordinates and isotropic displacement parameters are listed in Tables S1 and S2 in Supporting Information. Detailed crystallographic information on the refinements of CaP_8N_{14} and SrP_8N_{14} is provided in Table S3. Further details on CaP_8N_{14} can be obtained from the Fachinformationszentrum Karlsruhe (FIZ) by quoting the deposition number CSD 1979592 via www.ccdc.cam.ac.uk/structures.

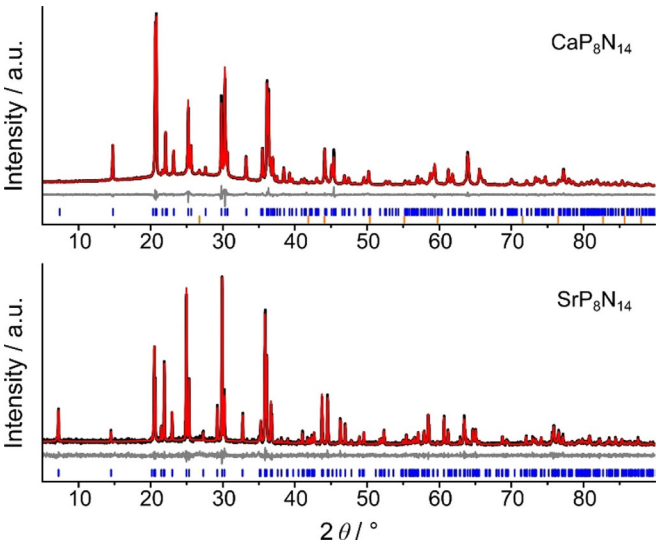

Figure 2. Rietveld refinements for CaP_8N_{14} and SrP_8N_{14}: observed (black, $Cu_{K_{\alpha 1}}$) and calculated (red) powder X-ray diffraction patterns are displayed with corresponding difference profiles (gray). Vertical blue bars mark the Bragg reflections of the title compounds, orange bars mark the Bragg positions of h-BN (crucible material) that appeared as a minor side phase of CaP_8N_{14}.

At first glance, the PXRD pattern of BaP_8N_{14} bears similarities with those of AEP_8N_{14} (AE = Ca, Sr) (Figure S1). However, corresponding Rietveld refinement did not yield reasonable results. Hence, a combination of transmission electron microscopy (TEM) and diffraction of microfocused synchrotron radiation was used for structure determination as described in previous works.[27,28] For this purpose, micron-sized crystals of BaP_8N_{14} were identified on a TEM grid by EDX analysis and selected area electron diffraction. Their precise positions were recorded (Figure S2) and single-crystal X-ray diffraction data were collected at the ESRF (beamline ID11) using a microfocused synchrotron beam (diameter ≈1×2 µm).

The crystal structure of BaP_8N_{14} was solved and refined in orthorhombic space group $Amm2$ (no. 38) with unit cell dimensions a = 12.4862(7), b = 8.6648(3) and c = 5.1373(2) Å. All atoms were refined anisotropically. Crystallographic data are summarized in the Supporting Information (Tables S4–S6) and can be obtained from the Fachinformationszentrum Karlsruhe

© 2020 The Authors. Published by Wiley-VCH Verlag GmbH & Co. KGaA, Weinheim

(FIZ) by quoting the deposition number CSD 1980141 via www.ccdc.cam.ac.uk/structures.

The refined structure model was used to verify the phase purity of BaP_8N_{14} by Rietveld refinement (Figure 3). More information on the Rietveld refinement for BaP_8N_{14} is provided in Table S7.

The chemical compositions of the title compounds were confirmed by energy-dispersive X-ray spectroscopy (EDX, Tables S8–S10). The spectra show trace amounts of oxygen, which may be attributed to partial surface hydrolysis during water treatment.

Fourier-transform infrared spectroscopy demonstrates the absence of N–H groups (Figures S4). The spectra feature only vibrations in the fingerprint region (400–1500 cm^{-1}) and do not indicate N–H valence modes.

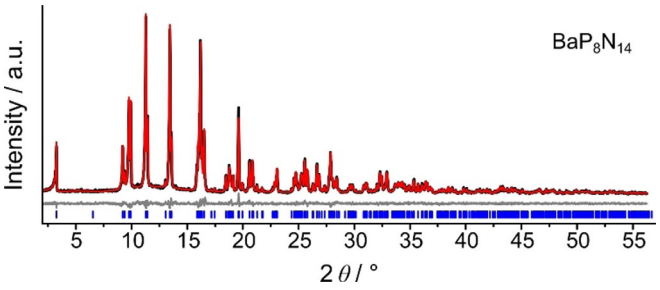

Figure 3. Rietveld refinement for BaP_8N_{14}:Eu^{2+}; observed (black, Mo_{K_α}) and refined (red) diffraction pattern. The difference profile is displayed in gray. Positions of Bragg reflections of BaP_8N_{14} are marked with vertical blue bars.

Structure description

The compounds AEP_8N_{14} (AE = Ca, Sr, Ba) can be classified as highly condensed nitridophosphates with a degree of condensation $\kappa = 8/14 \approx 0.57$, which is defined by the ratio of tetrahedra centres $n(P) = 8$ to the number of N atoms $n(N) = 14$. All title compounds feature quadruple layers that are separated by metal atoms (Figure 4). A more detailed description of the layered structure is provided in literature and the Supporting Information (Figure S5).[20] The structure types of AEP_8N_{14} (AE = Ca, Sr) and BaP_8N_{14} differ with respect to the stacking pattern of the quadruple layers. In CaP_8N_{14} and SrP_8N_{14}, these layers are related by rotation according to a 2_1 screw axis along [0 0 1] and by inversion symmetry. In the non-centrosymmetric structure of BaP_8N_{14}, however, they are related by a mirror plane ∥ (0 0 1) (Figure 4), resulting in a unit cell with half volume.

In CaP_8N_{14} and SrP_8N_{14}, the alkaline earth atom occupies one crystallographic site, that is octahedrally coordinated by N atoms with mean interatomic distances AE–N of 2.55 and 2.70 Å, respectively. In contrast, Ba occupies one crystallographic site, as well, but is located in a trigonal-prismatic coordination with a mean interatomic Ba–N distance of 2.83 Å. All observed AE–N distances are in good agreement with values of other known nitridophosphates as well as with the sums of the ionic radii.[15,17,18,20,29–31] This change of the coordination sphere is reminiscent of the $AEH_4P_6N_{12}$ (AE = Mg, Ca, Sr) compounds.[20,30] More detailed information on the coordination spheres in AEP_8N_{14} is provided in the Supporting Information (Figure S6 and Tables S11–S13).

For all title compounds, the P–N distances and N-P-N angles vary between 1.540(2)–1.737(4) Å and 103.1(2)–122.2(1)°, respectively, which is in good agreement with other nitridophosphates (Tables S11–S13).[15,17,18,20,29–31] The P–N distances dominate the coordination environments for N atoms with shorter distances for P–N[2] and slightly larger ones for P–N[3].[32]

Temperature dependent X-ray diffraction (HTXRD)

For the highly condensed nitridophosphates AEP_8N_{14} (AE = Ca, Sr, Ba), significant thermal stability can be expected, considering the highly covalent character of the P–N network. Therefore, temperature dependent X-ray diffraction was carried out between room temperature and 950 °C (Figures S7–S9). The

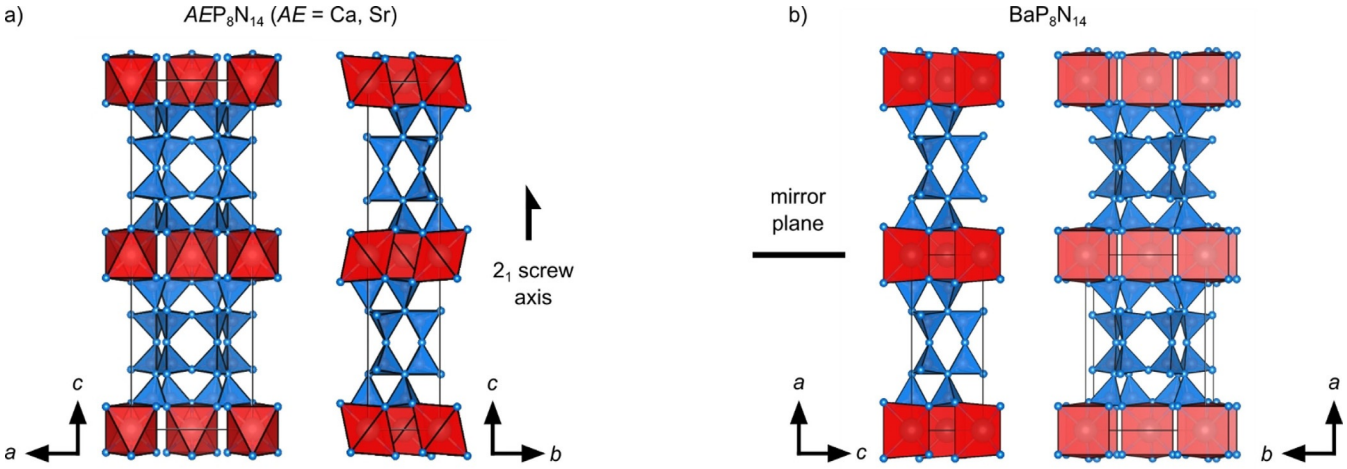

Figure 4. a) Projection of the crystal structure of AEP_8N_{14} (AE = Ca, Sr) along [0 1 0] and [1 0 0]; b) projection of the crystal structure of BaP_8N_{14} along [0 1 0] and (approximately) [0 0 1]. The structural relation of neighbouring quadruple layers is indicated by the respective symmetry elements. PN_4 tetrahedra are displayed in blue, AEN_6 polyhedra in red. N atoms are depicted as blue spheres.

© 2020 The Authors. Published by Wiley-VCH Verlag GmbH & Co. KGaA, Weinheim

compounds are stable over this temperature range and diffraction patterns show nothing but a linear increase of lattice parameters (Figures S7–S12). A quantification of the respective thermal expansion was derived by Rietveld refinements for selected temperatures. It reveals an increase in volume of 1.0% to 1.8% with respect to ambient temperature (Tables S14 and S15).

Luminescence

Considering the structural features as well as the chemical and thermal stability, AEP_8N_{14} (AE = Ca, Sr, Ba) appeared as promising host materials for phosphors, and thus were doped with Eu^{2+} (nominal ≈3 mole% referred to AE^{2+}) to investigate their luminescence properties. Upon excitation with near-UV to blue light, particles of all compounds show blue emission. Figures 5a and b show the excitation and emission spectra for $CaP_8N_{14}:Eu^{2+}$ and $SrP_8N_{14}:Eu^{2+}$, respectively. According to a single crystallographic site for AE^{2+}, on which Eu^{2+} is expected to be localized, both compounds show only one emission band. Corresponding emission wavelengths ($\lambda_{em}(CaP_8N_{14}:Eu^{2+})$ = 470 nm; $\lambda_{em}(SrP_8N_{14}:Eu^{2+})$ = 440 nm) are comparable with other alkaline earth nitridophosphates, for example, $BaP_2N_4:Eu^{2+}$ (λ_{em} = 454 nm), despite the different coordination spheres of the activator ions (Table 1). Considering the fwhm of 1380 cm^{-1} (31 nm) and 1350 cm^{-1} (26 nm), respectively, $CaP_8N_{14}:Eu^{2+}$ and $SrP_8N_{14}:Eu^{2+}$ can be classified as the first P/N-based ultra-narrow-band blue emitters and can compete with related (oxo)nitridoberyllate and —silicate phosphors.[4,11–13]

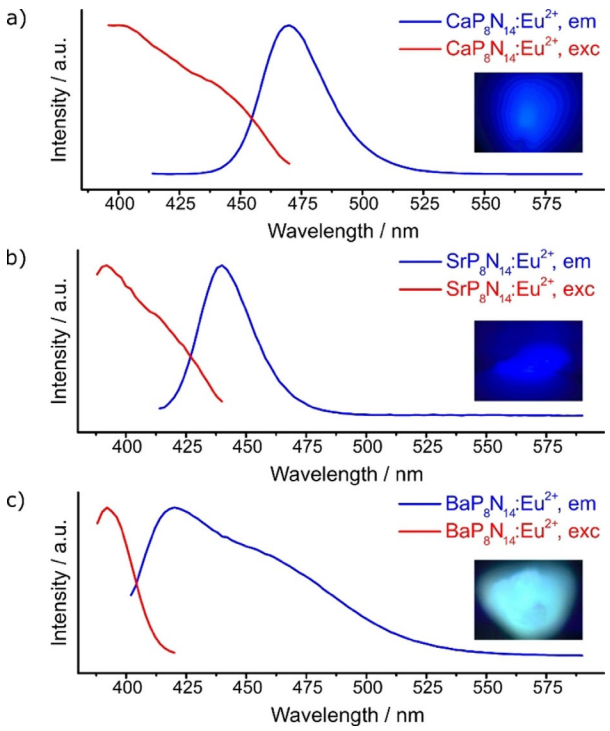

Figure 5. Normalized excitation (red) and emission spectra (blue) of $CaP_8N_{14}:Eu^{2+}$ (a), $SrP_8N_{14}:Eu^{2+}$ (b), and $BaP_8N_{14}:Eu^{2+}$ (c) measured at room temperature with respective micrographs of the measured crystals; $\lambda_{exc}(CaP_8N_{14}:Eu^{2+}, SrP_8N_{14}:Eu^{2+})$ = 400 nm, $\lambda_{exc}(BaP_8N_{14}:Eu^{2+})$ = 390 nm.

Table 1. Comparison of the luminescence properties at room temperature of $AEP_8N_{14}:Eu^{2+}$ (AE = Ca, Sr, Ba) with selected blue-emitting Eu^{2+}-doped (oxo)nitride materials.

Compound	*CN*	λ_{em} [nm]	λ_{exc} [nm]	Fwhm [nm]	Fwhm [cm^{-1}]	Reference
CaP_8N_{14}	6	470	400	31	1380	This work
SrP_8N_{14}	6	450	400	26	1350	This work
BaP_8N_{14}	6	417 457	390	36 ≈74	2075 3550	This work
BaP_2N_4	12	454	400	47	2244	[15]
$BaSr_2P_6N_{12}$	12	456	400	47	2240	[15]
$BaP_6N_{10}NH$	13	460	420	52	2423	[28]
$SrSi_6N_8$	10	450	370	44	–	[37]
$SrBe_{20}N_{14}$	12	428 540	380	22 >100	1180 –	[11]
$BaBe_{20}N_{14}$	12	426 530	380	25 >110	1310 –	[11]
$SrBe_6ON_4$	10	495	–	35	1400	[12]
$SrLi_2Be_4O_6$	8	456	400	25	1200	[13]
$BaLi_2Be_4O_6$	8	454	400	25	1200	[13]
$Sr_{0.25}Ba_{0.75}Si_2O_2N_2$	8	472	400	36	–	[4]
$BaSi_2O_2N_2$	8	492	450	37	–	[5]

In contrast to $CaP_8N_{14}:Eu^{2+}$ and $SrP_8N_{14}:Eu^{2+}$, $BaP_8N_{14}:Eu^{2+}$ shows a rather broad emission band at 417 nm (fwhm = 36 nm/2075 cm^{-1}) next to a significantly wider band at ≈457 nm (fwhm = 74 nm/3350 cm^{-1}, Figure 5c). In order to elucidate the maxima and fwhm of this emission, the spectrum was deconvoluted with two pseudo-Voigt functions (Figure S13; λ_{em1} = 417 nm, $fwhm_1$ = 36 nm/2075 cm^{-1} λ_{em2} = 457 nm, $fwhm_2$ = 74 nm/3350 cm^{-1}). The position of the first band fits well to the series of $AEP_8N_{14}:Eu^{2+}$ (AE = Ca, Sr) and is assigned to the one Ba site in BaP_8N_{14}. The second emission band can be explained by the comparison of the excitation spectra monitored at different wavelengths (λ_{mon} = 425–516 nm; Figure S14). Due to the very similar spectra for different λ_{mon}, the second emission band can unambiguously be assigned to the title compound as well, indicating large Stokes shifted impurity trapped exciton emission. Similar effects have already been observed for Ba compounds in literature.[33] The assumption that this artefact might be caused by a side phase can be excluded, as the emission band was observed in several phase-pure samples (Figure S15). The different relative intensities of the two emission bands in the different samples are most likely attributable to different excitation wavelengths (Figure S15). Characteristic parameters of the luminescent properties of $AEP_8N_{14}:Eu^{2+}$ (AE = Ca, Sr, Ba) are listed in Table 1, providing a brief comparison with other relevant blue phosphors.

Conclusions

In this contribution, we report on syntheses of the highly condensed nitridophosphates AEP_8N_{14} (AE = Ca, Sr, Ba) and illustrate their structural relation. Although all three compounds feature quadruple layers separated by metal atoms, only

© 2020 The Authors. Published by Wiley-VCH Verlag GmbH & Co. KGaA, Weinheim

SrP_8N_{14} and CaP_8N_{14} proved isotypic. The structure of BaP_8N_{14} as refined from diffraction data using microfocused synchrotron radiation differs in the orientation of these layers. Here, the layer stacking leads to a trigonal-prismatic environment of Ba^{2+}, while Ca^{2+} and Sr^{2+} are coordinated in octahedral fashion. Corresponding luminescence investigations on Eu^{2+}-doped samples show blue emission upon excitation with UV to blue light. The extremely narrow emission bands of CaP_8N_{14}:Eu^{2+} and SrP_8N_{14}:Eu^{2+} render these compounds competitive phosphors in comparison with other established classes of compounds. Especially, the Ca compound with its small Stokes shift shows very attractive luminescence properties for an application in solid-state lighting, because the lowest lying absorption band matches very well in spectral position with blue emitting InGaN LEDs. Hence, the spectral emission intensity distribution can lower the spectral gap between blue pump LED and green phosphor emission which is typically being observed in state-of-the-art white pc-LEDs. Filling this „cyan gap" of a white spectrum will significantly enhance colour rendition of a light source.[34,35] Moreover, pronounced thermal stability and absence of toxic elements further highlight the great potential of the AEP_8N_{14}:Eu^{2+} compounds. Future studies may thus focus on an alternative synthetic access in order to provide the preconditions for industrial application. Ammonothermal synthesis appears promising, as such syntheses of partially crystalline SrP_8N_{14} have already been reported.[36] Moreover, such methods could provide sufficient sample quantities for a more precise characterization of the luminescence performance, meaning for example, temperature-dependent emission spectra.

Experimental Section

Synthesis of P_3N_5: P_3N_5 was synthesized by ammonolysis starting from P_4S_{10} (ca. 7.0 g, Sigma Aldrich 99.99%) in a tube furnace lined with a silica tube. The apparatus, including the silica reaction boat, was heated for 4 h at 1000 °C under vacuum ($\leq 10^{-3}$ mbar) for drying. Subsequently, the starting material was loaded into the reaction boat under Ar flow. Only a limited amount of P_4S_{10} can be used, as otherwise the reaction tube may be clogged by by-products. After saturating the atmosphere in the silica tube for 4 h with a constant flow of dried NH_3 ($\approx$3.6 L h^{-1}, Air Liquide 5.0), P_4S_{10} was heated to 850 °C (rate: 5 °C min^{-1}) and held at this temperature for 4 h. Finally, the furnace was allowed to cool down to room temperature (rate: 5 °C min^{-1}) and the apparatus was flushed with Ar for 1 h in order to remove remaining NH_3. The recovered product showed orange coloured grains, which were purified by washing with water, ethanol, and acetone. Further information on the synthesis are given in literature.[38–40] P_3N_5 was identified by powder X-ray diffraction and FTIR spectroscopy.

Synthesis of $AE(N_3)_2$ (AE = Ca, Sr, Ba): Alkaline earth azides $AE(N_3)_2$ (AE = Ca, Sr, Ba) were synthesized by reactions of the respective alkaline earth carbonates ($CaCO_3$: Alfa Aesar, 99.5%; $SrCO_3$: Sigma Aldrich, 99.995%; $BaCO_3$: Grüssing, 99.8%) with HN_3 prepared by means with a cation exchanger (Amberlyst 15) according to the procedure described by Suhrmann and modified by Karau.[38,41] A diluted solution of HN_3 is formed in situ by passing an aqueous solution of NaN_3 (Acros Organics, 99%, extra pure) through the cation exchanger. HN_3 then drops into a stirred aqueous suspension of the carbonate until the eluate shows a neutral pH value and the solution turns clear. Residues of the carbonate were filtered off and the solvent was removed with a rotary evaporator (50 mbar, 40 °C). The products were obtained as colourless fine powders, which were recrystallized from acetone and dried under vacuum. $AE(N_3)_2$ (AE = Ca, Sr, Ba) were investigated for purity by powder X-ray diffraction and FTIR spectroscopy. **Caution**: Since HN_3 is potentially explosive and highly poisonous in its gaseous form, special care is necessary.

Synthesis of AEP_8N_{14} (AE = Ca, Sr, Ba): The nitridophosphates AEP_8N_{14} (AE = Ca, Sr, Ba) were obtained by high-pressure high-temperature synthesis using a 1000 t press with a modified Walker-type multianvil apparatus.[22–26] All products were synthesized from stoichiometric amounts of P_3N_5 and the respective alkaline earth azide (see Supporting Information, Table S16). Owing to the high air-sensitivity of the azides, the starting materials were handled in an Ar-filled glovebox (Unilab, MBraun, Garching, $O_2 < 1$ ppm, $H_2O <$ 0.1 ppm) and ground thoroughly in an agate mortar. The mixture was transferred into a cylindrical crucible made from hexagonal boron nitride (HeBoSint® S100, Henze, Kempten, Germany) and sealed with a boron nitride cap. The crucible was then placed in a specially prepared octahedron (MgO, doped with Cr_2O_3 (5%), edge length 18 mm, Ceramic Substrates & Components, Isle of Wight, UK), which was drilled through and loaded with different components. First, a ZrO_2 sleeve (Cesima Ceramics, Wust-Fischbeck, Germany) was fixed in the borehole and closed on one side by a Mo plate. Then, a long graphite tube (Schunk Kohlenstofftechnik GmbH, Gießen, Germany), a MgO spacer (Cesima Ceramics, Wust-Fischbeck, Germany) and a short graphite tube were put into the octahedron. While ZrO_2 served as thermal insulator, the two graphite tubes were used as electrical resistance furnace, whereby the combination of two single tubes is necessary to decrease the temperature gradient. After inserting the crucible with the sample, the assembly was completed by adding a second MgO spacer and a further Mo plate to ensure a symmetric setup. In order to generate approximately hydrostatic conditions, the uniaxial force of the hydraulic press was converted by a Walker-type module with inserted steel wedges, forming a cubic cavity. This cavity was filled by eight Co-doped (7%) WC cubes (Hawedia, Marklkofen, Germany). To enclose the sample octahedron, the edges of the WC cubes were truncated (11 mm edge length). Furthermore, four of the cubes were equipped with a PTFE film (Vitaflon Technische Produkte GmbH, Bad Kreuznach, Germany) for electrical insulation. The remaining cubes were prepared with pyrophyllite gaskets (Cermaic Substrates & Components, Isle of Wight, UK) to prevent the outflow of the MgO octahedron. Bristol board (369 g m^{-2}) was used to fix the gaskets. Further information on the experimental high-pressure setup is given in the literature.[42] Different pressure and temperature settings were used (CaP_8N_{14}: 5 GPa, $\approx$1075 °C; SrP_8N_{14}: 5 GPa, $\approx$1075 °C; BaP_8N_{14}: 4 GPa, $\approx$1150 °C). Detailed programs are given in Table S17.

Scanning electron microscopy (SEM) and energy-dispersive X-ray diffraction (EDX): The morphology of the samples was investigated with a Dualbeam Helios Nanolab G3 UC (FEI, Hillsboro). An X-Max 80 SDD EDX detector (Oxford Instruments, Abingdon) was used for chemical analyses. An adhesive carbon film was used to fix the samples on a holder. To ensure electrical conductivity, the samples were coated with carbon with an electron beam evaporator (BAL-TEC MED 020, Bal Tec AG). Data were analyzed with the Aztec software.[43]

Transmission electron microscopy (TEM): The sample was ground in an agate mortar, suspended in ethanol and drop-cast on a copper grid with holey carbon film (S160NH2C, Plano GmbH, Wet-

© 2020 The Authors. Published by Wiley-VCH Verlag GmbH & Co. KGaA, Weinheim

zlar, Germany). The grid was mounted on a double-tilt holder and isolated crystallites of BaP_8N_{14} were identified by EDX and electron diffraction using a FEI Tecnai G20 transmission electron microscope (TEM) with a thermal emitter (LaB_6) operated at 200 keV. Selected area electron diffraction patterns and bright-field images were recorded using a TVIPS camera (TemCam F216, Tietz) with a resolution of 2048×2048 pixels.

Single-crystal X-ray diffraction: The TEM grid was mounted on a Symétrie Hexapods Nanopos device. A BaP_8N_{14} crystal of about 2×3×0.5 μm in size was recovered at beamline ID11 ($\lambda = 0.309$ Å, ESRF, Grenoble) by a telescope with large magnification, using the copper crossbars of the grid as landmarks. The crystallite was centred using Ba X-ray fluorescence scans. The single-crystal data set was then collected using a microfocused synchrotron beam of 1×2 μm. CrysAlisPro and SADABS were used for the integration and the semiempirical absorption correction of the data.[44,45] The incomplete absorption of X-ray radiation in the CCD phosphor was corrected.[46] The crystal structure was solved by direct methods and refined by least-squares methods with SHELX-2014.[47]

CCDC 1979592 (Ca) and 1980141 (Ba) contain the supplementary crystallographic data for this paper. These data are provided free of charge by The Cambridge Crystallographic Data Centre through the CCDC/FIZ Karlsruhe joint deposition service.

FTIR spectroscopy: FTIR spectra of the title compounds were collected on a Spectrum BX II spectrometer (PerkinElmer, Waltham, MA, USA) between 600 and 4000 cm^{-1} with DuraSampler attenuated total reflectance unit (ATR).

Powder X-ray diffraction: Powder X-ray diffraction data were collected with a Stoe Stadi P diffractometer with $Cu_{K_{\alpha1}}$ ($\lambda = 1.5406$ Å) or $Mo_{K_{\alpha1}}$ ($\lambda = 0.71073$ Å) radiation. The diffractometers were equipped with Ge(111) monochromators and Mythen 1 K Si strip detectors (Dectris, Baden, Switzerland). The ground samples were transferred into glass capillaries with 0.3 mm diameter (Hilgenberg GmbH, Malsfeld, Germany). The TOPAS Academic 6.1 package was used for Rietveld refinements using the fundamental parameters approach and a shifted Chebyshev function for handling the background.[48] Temperature dependent powder X-ray diffraction data were collected on a Stoe Stadi P diffractometer ($Mo_{K_{\alpha1}}$ radiation; Ge(111) monochromator) with a resistance graphite furnace (Stoe) and IP-PSD detector. Samples were loaded into fused silica capillaries (0.5 mm diameter) and heated from room temperature to 950 °C with steps of 25 °C and a heating rate of 10 °C min^{-1}. At each step data were collected with constant temperature.

Luminescence: Luminescence spectra of Eu^{2+}-doped samples (≈3 mole%) were examined on a HORIBA Fluoromax4 spectrofluorimeter system with Olympus BX51 microscope. Emission spectra were collected at room temperature with $\lambda_{exc} = 400$ nm for AE = Ca, Sr, and $\lambda_{exc} = 390$ nm for Ba, respectively, in a range from 400 to 800 nm (step width: 2 nm). Excitation spectra were recorded with monitoring wavelength λ_{mon} from 425 to 516 nm.

Acknowledgements

We thank Lisa Gamperl (Department of Chemistry at LMU) for EDX measurements. Furthermore, we thank Volker Weiler (Lumileds Phosphor Center Aachen) for luminescence measurements. We also thank the ESRF, Grenoble, for granting beam time (project CH-5149) and the Deutsche Forschungsgemeinschaft (DFG) for financial support (projects OE 530/6-1 and SCHN 377/18-1). Dr. Christopher Benndorf, Markus Nentwig and Christina Fraunhofer are acknowledged for support during the beamtime.

Conflict of interest

The authors declare no conflict of interest.

Keywords: high-pressure chemistry · high-temperature chemistry · luminescence · microfocused synchrotron radiation · nitridophosphates

[1] P. Pust, P. J. Schmidt, W. Schnick, *Nat. Mater.* **2015**, *14*, 454–458.
[2] A. A. Setlur, *Electrochem. Soc. Interface* **2009**, *18(4)*, 32–36.
[3] Y. Shimizu, K. Sakano, Y. Noguchi, T. Moriguchi, *Light emitting device having a nitride compound semiconductor and a phosphor containing a garnet fluorescent material*, **1999**, US Patent 5998925 A.
[4] M. Seibald, T. Rosenthal, O. Oeckler, F. Fahrnbauer, A. Tücks, P. J. Schmidt, W. Schnick, *Chem. Eur. J.* **2012**, *18*, 13446–13452.
[5] J. A. Kechele, O. Oeckler, F. Stadler, W. Schnick, *Solid State Sci.* **2009**, *11*, 537–543.
[6] H. A. Höppe, H. Lutz, P. Morys, W. Schnick, A. Seilmeier, *J. Phys. Chem. Solids* **2000**, *61*, 2001–2006.
[7] Y. Q. Li, J. E. J. van Steen, J. W. H. van Krevel, G. Botty, A. C. A. Delsing, F. J. DiSalvo, G. de With, H. T. Hintzen, *J. Alloys Compd.* **2006**, *417*, 273–279.
[8] S. Schmiechen, H. Schneider, P. Wagatha, C. Hecht, P. J. Schmidt, W. Schnick, *Chem. Mater.* **2014**, *26*, 2712–2719.
[9] K. Uhedaa, N. Hirosakib, Y. Yamamotob, A. Naitoa, T. Nakajimaa, H. Yamamotoa, *Electrochem. Solid-State Lett.* **2006**, *9*, H22–H25.
[10] P. Pust, V. Weiler, C. Hecht, A. Tücks, A. S. Wochnik, A.-K. Henß, D. Wiechert, C. Scheu, P. J. Schmidt, W. Schnick, *Nat. Mater.* **2014**, *13*, 891–896.
[11] E. Elzer, R. Niklaus, P. J. Strobel, V. Weiler, P. J. Schmidt, W. Schnick, *Chem. Mater.* **2019**, *31*, 3174–3182.
[12] P. Strobel, T. de Boer, V. Weiler, P. J. Schmidt, A. Moewes, W. Schnick, *Chem. Mater.* **2018**, *30*, 3122–3130.
[13] P. Strobel, C. Maak, V. Weiler, P. J. Schmidt, W. Schnick, *Angew. Chem. Int. Ed.* **2018**, *57*, 8739–8743; *Angew. Chem.* **2018**, *130*, 8875–8879.
[14] S. D. Kloß, W. Schnick, *Angew. Chem. Int. Ed.* **2019**, *58*, 7933–7944; *Angew. Chem.* **2019**, *131*, 8015–8027.
[15] F. J. Pucher, A. Marchuk, P. J. Schmidt, D. Wiechert, W. Schnick, *Chem. Eur. J.* **2015**, *21*, 6443–6448.
[16] M. Mallmann, S. Wendl, P. Strobel, P. J. Schmidt, W. Schnick, *Chem. Eur. J.* https://doi.org/10.1002/chem.202000297.
[17] A. Marchuk, W. Schnick, *Angew. Chem. Int. Ed.* **2015**, *54*, 2383–2387; *Angew. Chem.* **2015**, *127*, 2413–2417.
[18] A. Marchuk, S. Wendl, N. Imamovic, F. Tambornino, D. Wiechert, P. J. Schmidt, W. Schnick, *Chem. Mater.* **2015**, *27*, 6432–6441.
[19] F. Karau, W. Schnick, *Z. Anorg. Allg. Chem.* **2006**, *632*, 231–237.
[20] S. Wendl, W. Schnick, *Chem. Eur. J.* **2018**, *24*, 15889–15896.
[21] W. Schnick, *Angew. Chem. Int. Ed. Engl.* **1993**, *32*, 806–818; *Angew. Chem.* **1993**, *105*, 846–858.
[22] H. Huppertz, *Z. Kristallogr.* **2004**, *219*, 330–338.
[23] N. Kawai, S. Endo, *Rev. Sci. Instrum.* **1970**, *41*, 1178–1181.
[24] D. C. Rubie, *Phase Transitions* **1999**, *68*, 431–451.
[25] D. Walker, *Am. Mineral.* **1991**, *76*, 1092–1100.
[26] D. Walker, M. A. Carpenter, C. M. Hitch, *Am. Mineral.* **1990**, *75*, 1020–1028.
[27] F. Fahrnbauer, T. Rosenthal, T. Schmutzler, G. Wagner, G. B. M. Vaughan, J. P. Wright, O. Oeckler, *Angew. Chem. Int. Ed.* **2015**, *54*, 10020–10023; *Angew. Chem.* **2015**, *127*, 10158–10161.
[28] S. Wendl, L. Eisenburger, M. Zipkat, D. Günther, J. P. Wright, P. J. Schmidt, O. Oeckler, W. Schnick, *Chem. Eur. J.* **2020**, *26*, 5010–5016.
[29] W. H. Baur, *Crystallogr. Rev.* **1987**, *1*, 59–83.
[30] A. Marchuk, V. R. Celinski, J. Schmedt auf der Günne, W. Schnick, *Chem. Eur. J.* **2015**, *21*, 5836–5842.
[31] R. Shannon, *Acta Crystallogr. Sect. A* **1976**, *32*, 751–767.

 © 2020 The Authors. Published by Wiley-VCH Verlag GmbH & Co. KGaA, Weinheim

[32] Superscripted numbers in square brackets following element symbols denote coordination numbers.
[33] P. Dorenbos, *J. Phys. Condens. Matter* **2003**, *15*, 2645 – 2665.
[34] J. J. Joos, J. Botterman, P. F. Smet, *J. Solid State Lighting* **2014**, *1*, 6.
[35] A. Piquette, W. Bergbauer, B. Galler, K. C. Mishra, *ECS J. Solid State Sci. Technol.* **2016**, *5*, R3146 – R3159.
[36] M. Mallmann, S. Wendl, W. Schnick, *Chem. Eur. J.* **2020**, *26*, 2067 – 2072.
[37] K. Shioi, N. Hirosaki, R.-J. Xie, T. Takeda, Y. Q. Li, *J. Mater. Sci.* **2008**, *43*, 5659 – 5661.
[38] F. W. Karau, Dissertation, Ludwig-Maximilians-Universität Menchen (Germany) **2007**.
[39] J. Lücke, Dissertation, Rheinische Friedrich-Wilhelms-Universität Bonn (Germany) **1994**.
[40] A. Stock, H. Grüneberg, *Ber. dtsch. Chem. Ges.* **1907**, *40*, 2573 – 2578.
[41] R. Suhrmann, K. Clusius, *Z. Anorg. Allg. Chem.* **1926**, *152*, 52 – 58.
[42] H. Huppertz, Habilitationsschrift, Ludwig-Maximilians-Universität München (Germany) **2003**.
[43] Oxford Instruments, *AZtecEnergy Vers. 3.1*, Abingdon, United Kingdom, **2016**.
[44] Agilent Technologies, *CrysAlis Pro*, Yarnton, Oxfordshire, England, **2011**.
[45] Bruker AXS, Inc., *SADABS*, Madison, Wisconsin, USA, **2001**.
[46] G. Wu, B. L. Rodrigues, P. Coppens, *J. Appl. Crystallogr.* **2002**, *35*, 356 – 359.
[47] G. M. Sheldrick, *Acta Crystallogr. Sect. C* **2015**, *71*, 3 – 8.
[48] A. A. Coelho, *TOPAS Academic*, Version 6, Coelho Software, Brisbane, Australia, **2016**.

Manuscript received: March 4, 2020
Accepted manuscript online: April 8, 2020
Version of record online: May 11, 2020

 © 2020 The Authors. Published by Wiley-VCH Verlag GmbH & Co. KGaA, Weinheim